SAND 75 0079
Unlimited Release

8184 File 1.5

Total Hemispherical Emittance Measurement Apparatus for Solar Selective Coatings

Richard B. Pettit
Thermophysical Properties Division

Prepared by Sandia Laboratories, Albuquerque, New Mexico 87115 and Livermore, California 94550 for the United States Energy Research and Development Administration under Contract AT (29-1)-789

June 1975

Sandia Laboratories
energy report

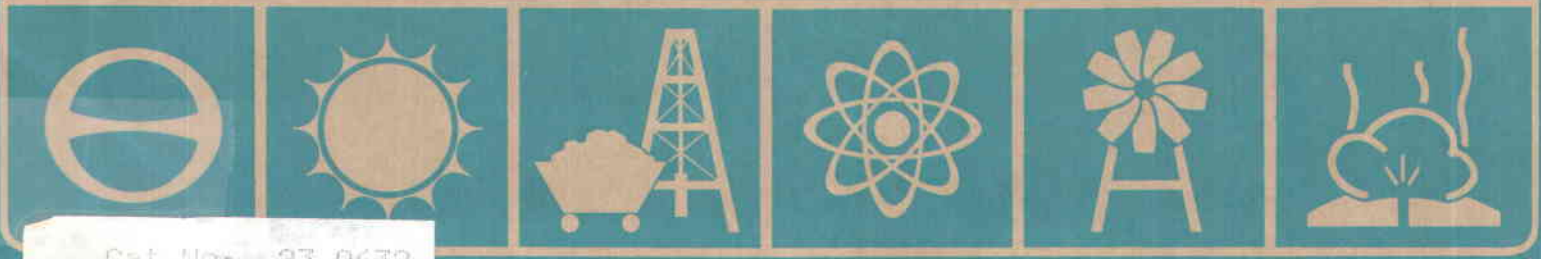

Issued by Sandia Laboratories, operated for the United States Energy Research and Development Administration by Sandia Corporation.

TOTAL HEMISPHERICAL EMITTANCE MEASUREMENT APPARATUS FOR SOLAR SELECTIVE COATINGS

SAND-75 0079

R. B. Pettit
Thermophysical Properties Division 5842

ABSTRACT

An apparatus designed to measure the total hemispherical emittance of solar selective coatings and metallic substrates over the temperature range 0°C to approximately 300°C is described. This apparatus utilizes a delta-power calorimetric measurement technique. After an error analysis is presented, emittance values of several metallic substrate materials are presented and compared with previous measurements.

TOTAL HEMISPHERICAL EMITTANCE MEASUREMENT APPARATUS FOR SOLAR SELECTIVE COATINGS

Introduction

The utilization of thermal energy derived from solar radiation using either a flat plate or a focused collector system requires an efficient solar selective coating.[1] An efficient coating is defined as having a high absorptance (α) over the solar spectrum[2] (approximately 0.30 to 2.0 μm) but in addition, having a low emittance (ϵ) to reduce thermal radiative heat losses (for moderate temperatures, this radiation occurs at wavelengths greater than 2 μm). (See Figure 1.) Therefore, a quantity that has been used to characterize solar selective coatings is the ratio of the solar absorptance coefficient (α_s) to the thermal emittance or the α_s/ϵ ratio. A good selective coating might be expected to have $\alpha_s/\epsilon \cong 10$. However, the main requirement should be to obtain α_s values as large as possible (e.g., with $\alpha_s \geq 0.95$ and $\epsilon \sim 0.10$).

There are a variety of techniques for preparing solar selective coatings.[3] One approach involves using a coating which is absorbing over the solar spectrum but which is transparent in the infrared.[4] In this case, the emittance is mainly controlled by the emittance of the substrate, which can be made very low by using a polished metal surface, for example. A second approach involves a careful control of the surface roughness such that solar radiation suffers multiple reflections and is absorbed, while for longer wavelength radiation the surface appears smooth and takes on the emittance of the base material.[3] Both approaches have been tried with success.[3,4]

In a heat transfer calculation of the performance of a solar collector system, the thermal radiation heat transfer is governed by the total hemispherical emittance ($\epsilon_{t,H}$).[5] The term <u>total</u> refers to an average over a blackbody wavelength distribution. Because this distribution is

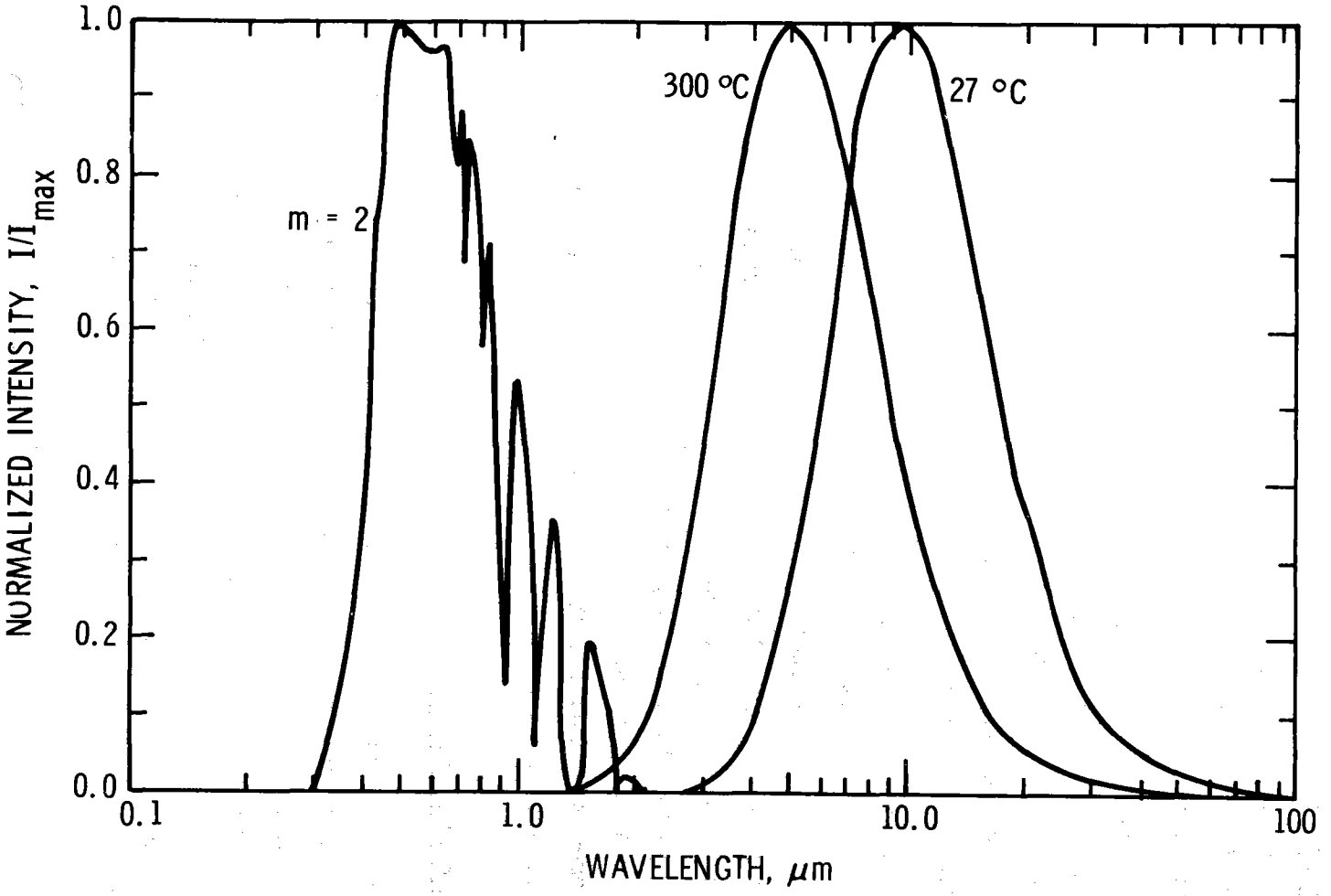

Figure 1. The normalized solar spectrum for air mass 2 as a function of wavelength together with normalized blackbody spectra at 27°C and 300°C. m is the effective air mass for the solar radiation (m = sec θ, where θ is the zenith angle of the sun. Thus, m=1 for the sun at zenith, etc.).

temperature dependent, the total emittance will be a temperature dependent property if the spectral emittance is not constant with wavelength. The term hemispherical refers to radiation over a complete hemisphere. For a flat plate collector system, one is interested in the emittance* from ambient to approximately 100°C, while for a focused collector, the upper temperature limit may be above 300°C.

Because the emittance is a surface property[6], it will depend upon the surface condition of the material, such as the surface roughness, surface films, oxide layers, etc. Therefore, it is important to be able to measure the emittance of uncoated substrates as well as the emittance of each coating-substrate combination.

The purpose of this report is to describe an apparatus designed to measure the total hemispherical emittance of solar selective coatings and low emittance metallic substrates over the temperature range from room temperature to approximately 300°C. After a brief discussion of several emittance measurement techniques, the present technique and apparatus are described and an error analysis is presented. Emittance values of several suitable metallic substrate materials are presented and compared with previous measurements. Finally, future improvements in the measurement technique are discussed.

Emittance Measurement Techniques

All the techniques used for absolute total hemispherical emittance measurements can be divided into two categories: calorimetric and reflectance techniques. The calorimetric techniques are considered the more accurate as well as more direct while the reflectance techniques are more rapid.[7,8] For a calorimetric measurement, a sample of known radiating surface area is placed in an environment where heat loss or gain is by radiant heat transfer only. The emittance is then computed from a knowledge of the amount of power (usually supplied by an internal electric heater) required to maintain the sample at a measured equilibrium temperature. This is called the steady-state

* From this point, the term emittance will mean the total hemispherical emittance unless otherwise noted.

technique. With a knowledge of the heat capacity of the specimen, the emittance can also be computed from a measurement of the rate of temperature change of the sample (the transient technique). If the input power is supplied by a solar simulator, then both the solar absorptance and the emittance as a function of temperature can be obtained.[9] In either case, the total hemispherical emittance is measured directly.

Reflectance techniques do not determine the total hemispherical emittance directly, but determine the emittance as a function of wavelength and incident angle. By averaging these data over the appropriate blackbody spectrum and angles, the total hemispherical emittance is obtained. The basis for measuring the emittance by reflectance techniques is Kirchhoff's Law, which states that the spectral emittance of an opaque material is equal to one minus the spectral reflectance.[10] In order to measure the reflectance of a non-specular surface, rather elaborate radiation collection devices are required (i.e., integrating spheres, paraboloids or ellipsoids).[8] For low emittance surfaces, small errors in the reflectance measurement become magnified when one calculates the emittance. For example, consider a surface with an emittance of 0.05; a 2% error in reflectance amounts to a 40% error in emittance. In addition, the lack of data for angles above 75° introduces an additional error of about $\pm$ 0.02 emittance units.[7] However, the reflectance techniques have the advantages of (1) fast acquisition of data, (2) simple sample geometry and mounting, and (3) spectral and angular emittance data.

A more detailed comparison of these emittance measurement techniques has been previously reported.[7] The method to be described in this report is a modification of the steady-state calorimetric technique.

Calorimetric Emittance Technique

For the calorimetric technique, the sample is placed in a vacuum chamber (to eliminate gas convection and conduction losses) as well as inside an isothermal chamber which is at a temperature much less than the sample temperature. Schematics of the present apparatus are shown in Figures 2 and 3. The liquid

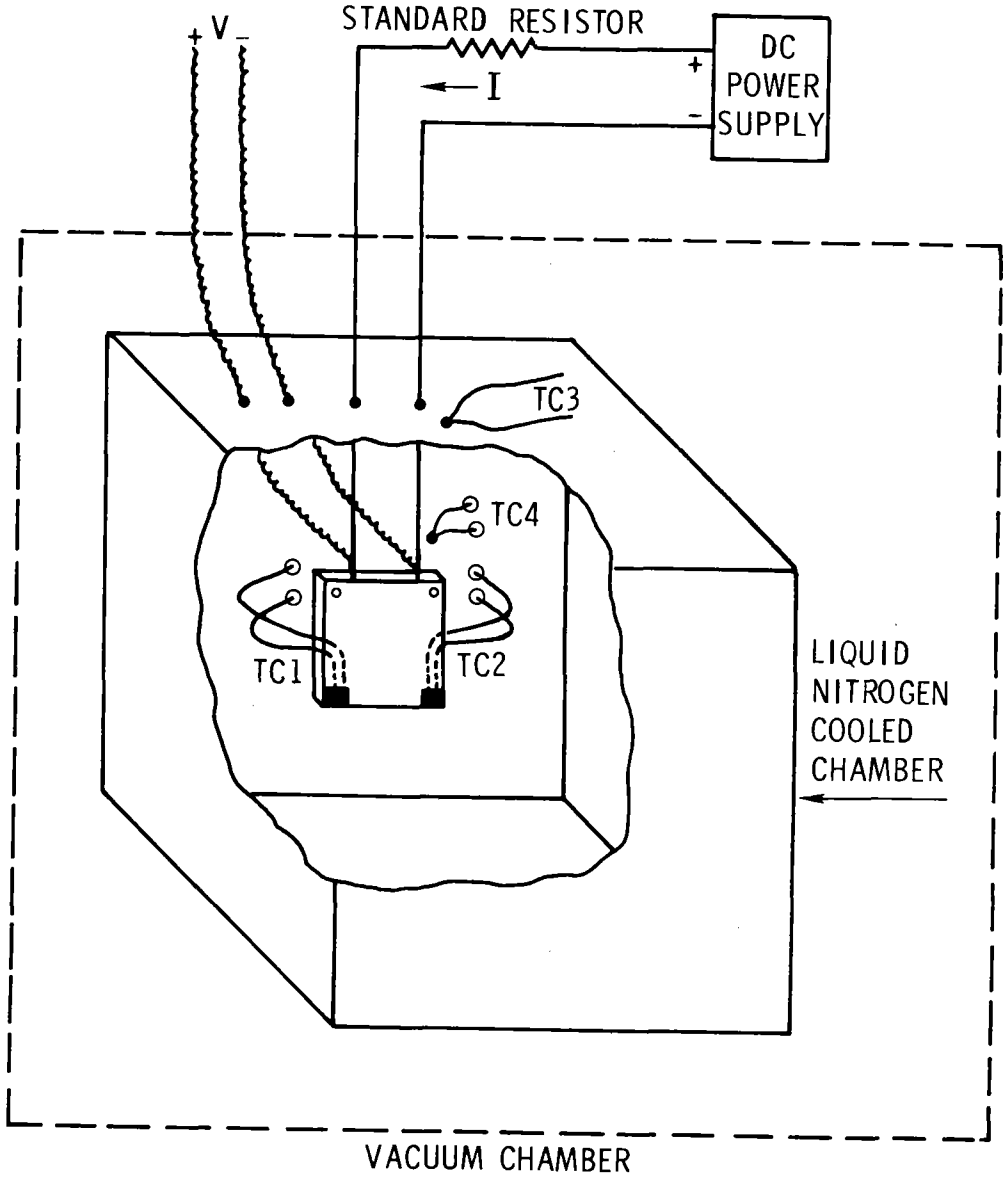

Figure 2. A schematic diagram of the total hemispherical emittance apparatus. Thermocouples marked TC1 and TC2 are located inside the sample, while TC3 is located on the chamber wall at a point above the sample and TC4 is located on the chamber wall directly opposite the sample.

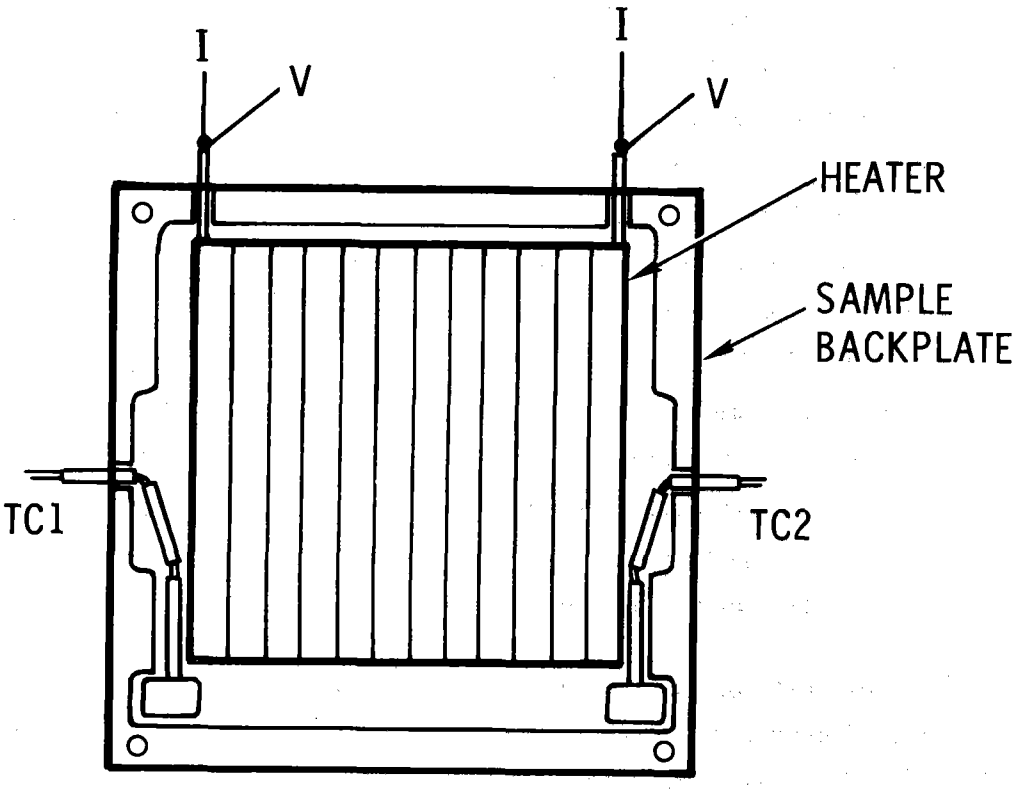

Figure 3. A scale drawing of the sample with the cover plate removed showing the location of the electric heater and two thermocouples TC1 and TC2.

nitrogen cooled copper chamber (dimensions 9" x 9" x 15" high) is painted on the inside with 3M-401 black velvet paint ($\varepsilon_{t,H} \geq 0.88$ from 77 K to 300°C.)[11] The sample itself is composed of two parts: (1) a back plate which has a machined cavity (0.085" deep) to accommodate an electric-heater together with two chromel-alumel thermocouples, and (2) a flat cover plate fitted with four countersunk holes to accommodate flat head machine screws. The heater is made from No. 28 Nichrome wire which is wrapped around an Al_2O_3 pressed sheet (0.030" thick) and cemented in place with high temperature ceramic cement. The resistance of the heater is about 54 Ω at room temperature. Both the heater and the inside surface of each sample are painted with Pyromark paint ($\varepsilon_{t,H} \geq 0.80$ from 25°C to 300°C)[12] to maximize thermal radiation heat transfer between the heater and the sample. Power to the heater is supplied by either a constant current or constant voltage DC regulated power supply. The current is monitored with a precision standard resistor, while the heater voltage is monitored with separate voltage measurement wires attached to the heater at a point slightly above the upper edge of the sample.

Before describing the measurement procedure, consider first the radiant heat exchange between two bodies, where body (1) is completely surrounded by body (2). The heat flow out of body (1) (Q_{out}) is given by[5]

$$Q_{out} = \frac{\sigma \varepsilon_1 A_1 (T_1^4 - T_2^4)}{1 + \frac{\varepsilon_1 A_1}{\varepsilon_2 A_2}(1 - \varepsilon_2)} \qquad (1)$$

where σ is the Stefan-Boltzmann constant, ε_1 and ε_2, A_1 and A_2, and T_1 and T_2 are the total hemispherical emittance, surface area, and temperature of bodies (1) and (2), respectively. It is interesting to note that in the limit $A_2/A_1 \to \infty$ or $\varepsilon_2 = 1.0$, the heat flow reduces to the simpler (and more familiar) equation

$$Q_{out} = \sigma \varepsilon_1 A_1 (T_1^4 - T_2^4) \left\{ \begin{array}{l} A_2/A_1 \to \infty \\ \text{and/or} \\ \varepsilon_2 = 1.0 \end{array} \right\} \qquad (2)$$

For the present apparatus, this equation can be used with little error because the ratio A_2/A_1 is large and $\epsilon_2 \geq 0.88$, as will be discussed later.

If a power, P_{in}, is being supplied to body (1) (by an electric heater, for example), then in equilibrium $P_{in} = Q_{out}$. By measuring the equilibrium temperature and surface area of the sample, as well as the temperature of the environment, equation (2) can be used to calculate the emittance of the sample. This is called the steady-state calorimetric technique. If the sample is not in equilibrium but is uniform in temperature, then the rate of change of the sample temperature follows the equation[9]

$$MC_p \frac{dT}{dt} = P_{in} - Q_{out} \tag{3}$$

where M is the sample mass, C_p is the specific heat of the sample, and t is the time. Thus, if one knows the heat capacity of the sample, heater, thermometers, etc., one can relate the power into the sample to its temperature and its rate of temperature change to determine the emittance. This is called the transient calorimetric technique. For this technique, the sample temperature can be either increasing or decreasing with time or the heater power can be zero (i.e., free cooling). In any case, one needs to know the effective specific heat of the sample as a function of temperature which usually limits the accuracy of the transient technique.

The major disadvantage of the steady-state technique is the large time constant and correspondingly long times required to reach equilibrium (or a point where $dT/dt \approx 0$). This is a particularly severe problem for low emittance samples. Considering equation (3) in more detail, we have

$$MC_p \frac{dT}{dt} = P_{in} - \sigma \epsilon A(T^4(t) - T_2^4) \tag{4}$$

where T_2 is the temperature of the sample environment. At equilibrium $dT/dt = 0$ and equation (4) defines the equilibrium temperature, T_{eq}, such that

$$T_{eq} = \left[\frac{P_{in}}{\epsilon \sigma A} + T_2^4\right]^{\frac{1}{4}} . \tag{5}$$

Solving this equation for the heater power, P_{in}, and substituting into equation (4) gives

$$MC_p \frac{dT(t)}{dt} = \sigma\epsilon A(T_{eq}^4 - T^4(t)) \tag{6}$$

If we assume that the sample is close to the equilibrium temperature such that $T(t) = T_{eq} - \Delta T(t)$, then we have

$$MC_p \frac{d\Delta T}{dt} = \sigma\epsilon A \left[4T_{eq}^3 \Delta T - \mathit{0}(T_{eq}^2 \Delta T^2)\right] \tag{7}$$

Neglecting terms of order ΔT^2 and higher, and solving for $\Delta T(t)$ we have

$$\Delta T = C\ e^{-t/\tau}$$

or

$$T(t) = T_{eq} - C\ e^{-t/\tau} \tag{8}$$

where C is a constant and

$$\tau = \frac{MC_p}{4\sigma\epsilon A\ T_{eq}^3} \tag{9}$$

Thus, the sample approaches equilibrium exponentially with time and the time constant is determined by the sample parameters as shown in equation (9). As an example of the time required to approach equilibrium as a function of the sample emittance and temperature, assume that at t=0, the sample is 15°C below the equilibrium temperature (for a copper sample of 133 cm^2 area and mass of 183 grams), then the time required to approach within 0.5°C of T_{eq} is shown in Table 1. As one can see, for a sample with an emittance of 0.20 or less, the time required to reach 0.5°C from the steady-state temperature is on the order of hours. Thus for low emittance samples, which happen to be the most important in terms of solar selective coatings, it would take several days to a week to obtain emittance data at 5 or 6 temperatures between ambient and 300°C.

Table I. Time for Temperature to Move from 15°C from Set Point to 0.5°C from Set Point as a Function of Sample Emittance and Temperature

Total Hemispherical Emittance	1.0	0.5	0.2	0.1	0.05
25°C	50 min	100 min	4.1 hr	8.2 hr	17 hr
100°C	26 min	52 min	2.2 hr	4.3 hr	8.7 hr
200°C	12.7 min	25 min	64 min	2.1 hr	4.2 hr
300°C	7.1 min	14 min	36 min	1.2 hr	2.4 hr

In order to reduce the time required to reach a steady-state condition, several approaches have been attempted. A temperature control system which varies the heater power is impractical because the time constant of the control electronics must be suitably matched to the time constant of each sample. Assuming that the sample emittance is unknown, which is usually the case, the time constant of the control system cannot be optimally set and severe temperature cycling can result. Curve fitting heating and cooling data requires a knowledge of the specific heat as previously mentioned. If one accurately knows MC_p as a function of temperature for the complete sample, heater and thermometer system, then this is an accurate as well as rapid measurement technique. However, if one is working with a variety of sample materials (i.e., electroplated metal substrates) or if high-speed, timed-interval data recording capabilities are not available, this technique may be unattractive.

The technique that has been developed is called the "delta-power calorimetric emittance technique." This is used once the sample is close to the desired temperature set point and the sample's temperature is not changing very rapidly with time. Referring to Figure 4, one first maintains a heater power level, P_1, such that the sample temperature is definitely increasing with time. Thus P_1 represents a power level which is higher than the power required to maintain equilibrium at this temperature. Next the heater power is reduced to a value P_2, which is less than 1% lower than P_1, such that the sample temperature decreases with time. (If the sample temperature continues to increase at P_2, the power is reduced by another 1% until the sample temperature decreases with time.) Thus, P_2 represents a heater power lower than the power required to maintain equilibrium at this temperature. In this way, the required equilibrium power is determined with an accuracy of better than $\pm$ 0.5%, while the corresponding sample temperature variation is not more than $\pm$ 0.2°C.

Finally, the heater power is returned to a value P_1 and the increasing sample temperature noted. This eliminates any uncertainty in the sample not responding correctly to heater power changes, which might occur if the power was changed too quickly after heating the sample rapidly to the "equilibrium" temperature.

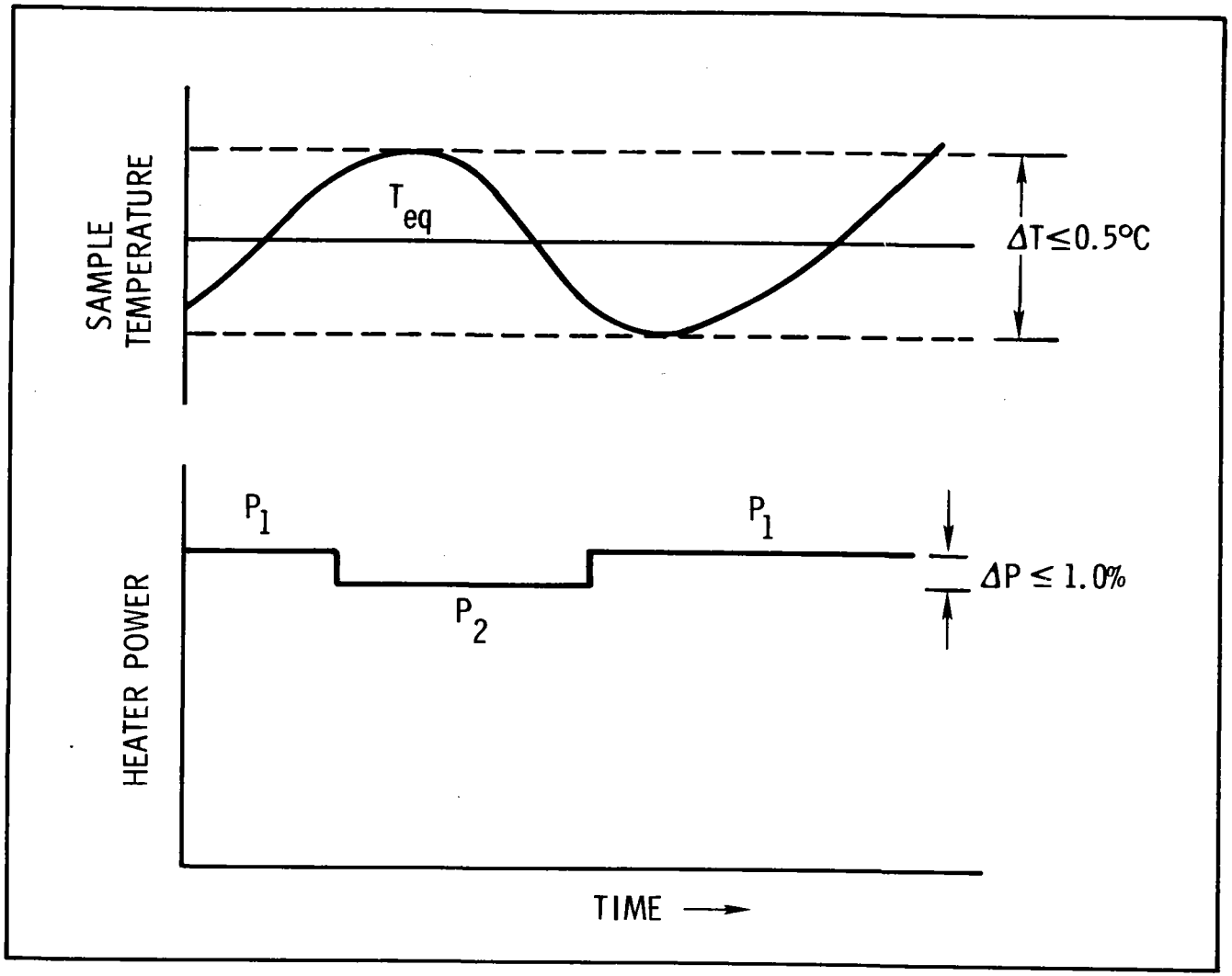

Figure 4. A representation of the sample temperature and heater power as a function of time when using the delta-power technique.

Using this technique, approximately 6 equilibrium temperatures can be obtained in two days for a sample with an emittance below 0.30, and in one day for higher emittance samples.

Error Analysis

An error analysis of the calorimetric technique must include the errors associated with all the quantities appearing in equation (2). In addition, because this technique depends upon the net heat radiated from the sample, a major source of error can be caused by heat transfer by other routes which must be compared to that radiated by the sample in order to determine the emittance error. Thus, referring to the thermal radiation heat transfer equation (2), Figure (2) and Figure (4), the sources of error include: (1) sample temperature measurement; (2) chamber temperature measurement; (3) thermal conduction losses and/or input from the thermocouple, voltage and heater wires; (4) heater power measurement; (5) sample area; (6) thermal gradients in the sample; (7) gas conduction and convection losses; and (8) the emittance and surface area of the chamber walls. Each of these losses is considered in detail below:

(1) Temperature Measurement: There are three distinct areas of temperature measurement error: (i) the intrinsic accuracy of the thermocouples, (ii) the uncertainty in achieving the equilibrium temperature, and (iii) assurance of good thermal contact between the sample and the thermocouples. The thermocouples used in the present apparatus are chromel-alumel, which have a accuracy of $\pm$ 2°C from 0°C to 277°C and 0.75% above 277°C. As previously discussed, for the delta-power technique, the equilibrium temperature is determined with a precision of $\pm$ 0.2°C for all temperatures. Thus at room temperature, the $\pm$ 2.2°C error corresponds to $\pm$ 2.9% emittance error, while at 300°C, the corresponding emittance error is $\pm$ 1.7%. Of possible greater importance in terms of the sample temperature measurement is ensuring good thermal contact between the thermocouples and the sample. Because the sample is in vacuum and the thermocouple wires are hot at the sample end and cold at the chamber wall, heat flow down the thermocouple leads can cool the thermocouple junction below the sample temperature resulting in erroneous temperature readings. Poor thermal contacts between the thermocouple and sample is evident most

distinctly during fast heat-up (or cool-down). In this case, a thermocouple in poor thermal contact lags behind a thermocouple in good thermal contact. By cementing the thermocouples in copper blocks which are then cemented into each sample (see Figure 3), the two thermocouple readings agree to within $\pm$ 1°C, which is well within their rated accuracy. In this way, thermal contact problems are reduced.

(2) Chamber Temperature: The temperature of the liquid nitrogen cooled chamber surrounding the sample is monitored by two thermocouples, one mounted above the sample and the other mounted opposite one flat side of the sample (see Figure 2). For room temperature samples, the maximum temperature of the chamber wall is 87°K, or about 10°K higher than the boiling point of LN_2. For high emittance samples at 300°C, the wall temperature opposite the sample increases to $\sim$ 95°K because of the heat input from the sample. Thus a sample at room temperature is in an environment at (82 $\pm$ 5)°K, which leads to an emittance error of $\pm$ 0.14%, while a sample at 300°C is in an environment at (86 $\pm$ 9)°K, which leads to an emittance error of $\pm$ 0.03%.

(3) Thermal Losses/Gains from TC, Heater and Voltage Wires: Thermal losses/gains from thermocouple (TC), heater or voltage wires can be calculated from a knowledge of the thermal conductivity, total hemispherical emittance, and resistivity of the material involved. If one considers an isolated portion of wire in a vacuum environment with a current I flowing through it, the heat loss or gain of a unit element dx in length at temperature T(x) is given by:

$$\frac{I^2\rho}{A} - KA\frac{d^2T}{dx^2} = \sigma\,\epsilon\,2\pi r\,(T^4(x) - T_{wall}^4) \qquad (10)$$

where K is the thermal conductivity, A is the cross-sectional area, ϵ is the total hemispherical emittance, r is the radius, and ρ is the electrical resistivity of the wire. If there is no current flowing in the wire, equation (10) can be integrated once to give:

$$\frac{dT}{dx} = \sqrt{\frac{4\pi\sigma}{5Kr}} \left\{ T^5(x) - 5T_w^4 T(x) + C \right\}^{\frac{1}{2}} \qquad (11)$$

where C is a constant. Assuming that the wire is semi-infinite in length, and that at the wall, $T=T_w$, and $dT/dx=0$, one obtains for the heat loss at the sample ($T=T_s$):[9]

$$Q = \sqrt{\frac{4\pi^2 K\epsilon\sigma r^3}{5}} \left\{ T_s^5 - 5T_w^4 T_s + 4T_w^5 \right\}^{\frac{1}{2}} \qquad (12)$$

However, for the general case of a finite length wire, L, with a current flowing through it, equation (10) must be solved numerically subject to the boundary conditions $T(x)=T_w$ at x=0, and $T(x)=T_s$ at x=L. For the particular case of a 12.6 mil diameter nichrome wire (K = 0.15 watts/cm-K, $\epsilon \sim 0.3$ and $\rho=1.5\times10^{-4}\Omega$-cm) at certain sample temperatures and current values, there will be heat flowing <u>into</u> the sample from the heater wires (i.e., the temperature at some point along the wire will be higher than T_s). For example, at T_s = 100°C, T_w = 77°K and L = 15 cm, at I = 0 A, the heat flow out of the sample is 8 mW while at a current I = 0.4 A, the heat flow into the sample is 28 mW (see Figure 5). It can be shown for the system reported here that the heat flow <u>into</u> the sample from the heater leads at maximum current is always less than or equal to the heat flow out of the sample from <u>all</u> leads for the case I = 0 A. Therefore, the maximum error in the overall heat loss or gain of the sample for the present apparatus has only to be calculated for the case I=0 A. In Table 2, the overall heat loss from four thermocouple wires (two chromel and two alumel, 0.005" dia.), two voltage wires (0.005" dia. nichrome) and two heater wires (0.0126" dia. nichrome) is tabulated as a function of the sample temperature. To obtain the corresponding emittance error, one must compare this heat loss with the heater power supplied to the sample, which is a function of the sample emittance and temperature.

(4) <u>Area Measurement</u>: The external dimensions of each sample are measured to within ± 0.001" after the emittance measurements have been performed. However, the sample thickness may vary by ± 0.005" depending

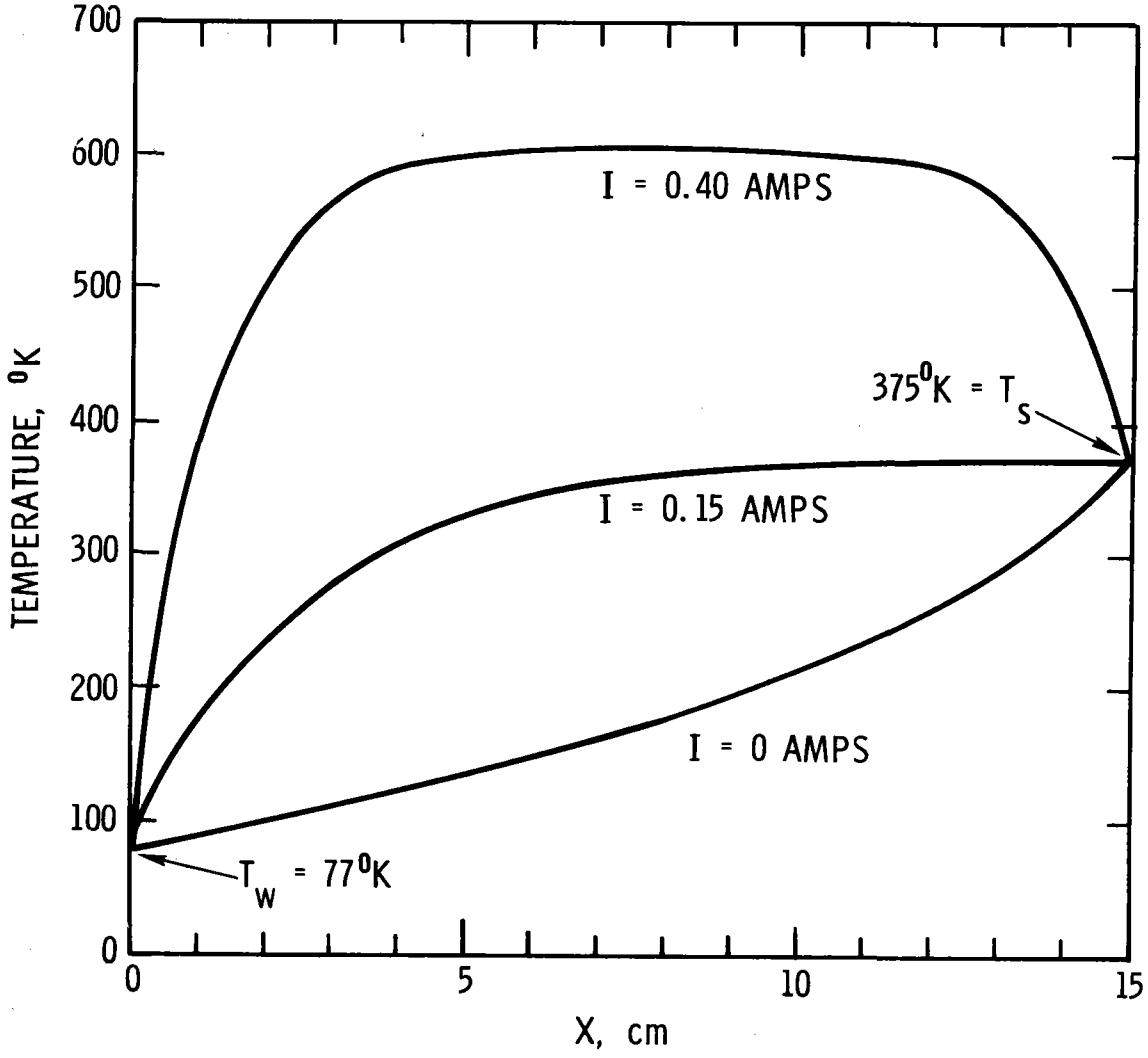

Figure 5. The temperature distribution along a wire whose ends are held at fixed temperatures of 77° K (typical wall temperature) and 373°K (typical sample temperature) for several values of the current.

upon the sample flatness and proper fitting of the heater and thermocouples. This leads to an uncertainty in the sample area of $\pm$ 0.35%. In addition, because of thermal expansion effects, the area is approximately 1% larger at 300°C than at room temperature. Thus the overall area uncertainty introduces an emittance error of $\pm$ 0.35% at 25°C and $\pm$ 1.35% at 300°C.

(5) Heater Power: The power into the heater in terms of the voltage and current readings themselves is measured with a precision of $\pm$ 0.1%. However, the voltage leads are by necessity located at a point slightly above the upper sample edge (see Figure 4). This introduces an increase in the correct voltage measurement of 1% $\pm$ 0.25% which is subtracted from all measured power readings. In addition, there is the $\pm$ 0.5% heater power uncertainty due to the delta-power technique. Thus the total uncertainty in the measured heater power is $\pm$ 0.85%.

(6) Temperature Gradients: Because the electric heater is not in perfect thermal contact with the sample, both the heater and the inside of the sample are painted black ($\epsilon_{t,H} \geq 0.90$) to maximize the thermal radiation exchange. Therefore, the heat input to the sample is uniform across the area of the sample subtended by the heater. Outside this area, there is no heat-input into the sample from the heater and a temperature gradient may exist at the edges of the sample. Assuming the worst case of a sample emittance of 1.0 at 300°C leads to a 0.1°C temperature difference for a copper sample (K = 3.85 W/cm-K), a 0.7°C difference for a 1018 steel sample (K = 0.52 W/cm-K) and a 2.4°C difference for 304 stainless steel (K = 0.18 W/cm-K). Thus for a substrate with a thermal conductivity above 0.5 W/cm-K, any temperature gradients are negligable compared with the temperature measurement uncertainty. Even for the stainless steel sample, the resulting emittance error is less than 1%.

(7) Gas Conduction: Gas conduction losses at our maximum operating pressure of 2×10^{-6} torr air are calculated from the formula[13]

$$Q = a\, A_s\, P_{\mu b}\, \Lambda \sqrt{\frac{273}{T_w}}\, (T_s - T_w) \qquad (13)$$

where a is a constant between 0 and 1, A_s is the sample surface area (133 cm^2), $P_{\mu b}$ is the pressure in microbars (1 $\mu b = 0.75 \times 10^{-3}$ torr), Λ = low pressure thermal conductivity of air ($= 1.21 \times 10^{-5} W\text{-}cm^2\text{-}K^{-1}\mu b^{-1}$). Thus at room temperature, Q = 1.6 mW while at 300°C, Q = 4.0 mW.

(8) Chamber Emittance and Area: The correct equation for calculating the emittance for the steady-state technique is equation (1). However, equation (2) can be used with little error. The chamber has an area of 4530 cm^2. The inside of the chamber is painted with 3M-401 black velvet paint which has an emittance of 0.88 or greater[11] from 77 K to 300°C. In using equation (2), the error is given by $\frac{\epsilon_1 A_1}{\epsilon_2 A_2}(1-\epsilon_2)$. For the parameters given above, the correction is 0.32% for a sample emittance of 1.0 and 0.03% for a sample emittance of 0.10.

All the above errors are listed in Table 2 for sample temperatures from room temperature to 300°C. The final absolute emittance error as a function of the sample temperature and emittance is shown in Figure 6. Thus, at room temperature for a sample with an emittance of 1.00, the error is $\pm$ 0.045 emittance units or $\pm$ 4.5% while with an emittance of 0.10, the error is $\pm$ 0.01 emittance units or $\pm$ 10%. Generally, for a sample emittance below 0.30, the error is below 0.02 emittance units.

A complete analysis of systematic errors has not been performed. Because the emittance is a surface dependent property, there are at present no emittance standards that can be used for absolute calibration purposes. However, data obtained for the same sample on two separate occasions agree to within 0.01 emittance units. In addition, data obtained on polished copper and electroplated gold samples agree with previously reported measurements, as indicated below.

Emittance Measurement Results

Using the emittance apparatus described above, emittance values have been obtained for a variety of metallic substrates both to characterize several base materials as solar coating substrates as well as to compare our measured values with previous data. As previously mentioned, many

Table II. Emittance Errors from Several Sources as a Function of the Sample Temperature from 25°C to 300°C

Source of Emittance Error	25°C	100°C	200°C	300°C
1) Sample Temperature	± 2.9%	± 2.3%	± 1.8%	± 1.7%
2) Chamber Temperature	± 0.14%	± 0.07%	± 0.04%	± 0.03%
3) Heat loss/gain(voltage, heater and thermocouple wires)*	± 20 mw	± 34 mw	± 62 mw	±100 mw
4) Area Measurement	± 0.35%	± 0.70%	± 1.0%	± 1.4%
5) Heater Power	± 0.85%	± 0.85%	± 0.85%	± 0.85%
6) Gas Conduction * (2×10^{-6} Torr)	- 1.6 mw	- 2.2 mw	- 3.0 mw	- 4.0 mw
7) Chamber area and emittance, (max error)	+ 0.3%	+ 0.3%	+ 0.3%	+ 0.3%

* Emittance errors from these sources are dependent upon sample emittance values and therefore are listed only as power losses or gains. See Figure 6 for total emittance errors.

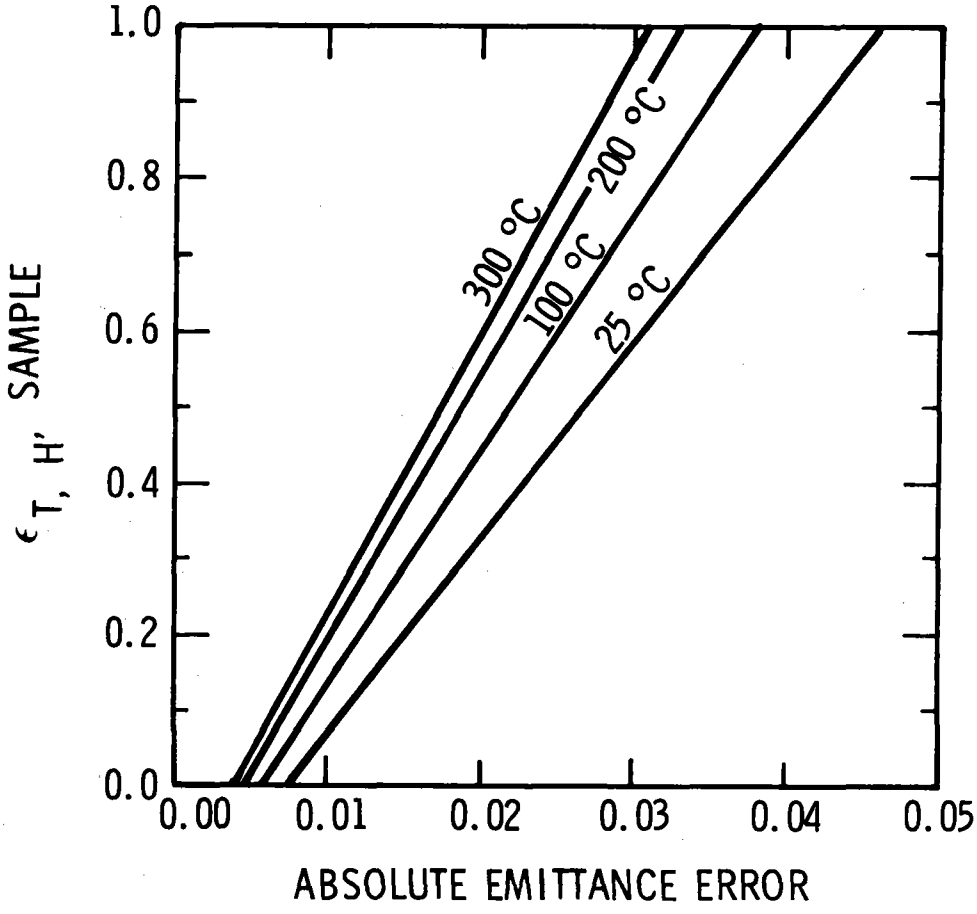

Figure 6. The absolute emittance error as a function of the sample emittance and temperature.

solar selective coatings are transparent in the infrared region so that the emittance depends upon the emittance of the substrate. In this way, a knowledge of the base metal emittance allows for an analysis of the effect of a selective coating which is independent of the substrate emittance. Furthermore, since the emittance of the metallic substrate may depend upon the surface roughness and preparation procedure, a measurement of the effect of various surface conditions on the emittance is important. Below is a listing of several metallic substrates that have been studied.

(1) OFHC Copper with a polished 8-microinch finish. The total hemispherical emittance varies from 0.03 at 25°C to 0.04 at 300°C. This agrees with analyzed data as compiled in the TPRC Data Series, Volume 7.[4] (See Figure 7a)

(2) Type 1018 mild steel with two surface finishes: (i) an 8-microinch ground finish and (ii) an 8-microinch ground finish plus a hand polish (Fig. 7a). The emittance of the polished sample is slightly lower than the emittance of the ground finished sample, as would be expected. It should be noted that mild steel is the proposed base material for the solar collector pipe.

(3) Type 304 stainless steel sample with a polished 8-microinch finish (Fig. 7a). The emittance varies from 0.12 at 25°C to 0.18 at 300°C. These data also agree with the limited data presented in the TPRC Data Series (Volume 7)[15], although large variations are reported there. The major drawback to using stainless steel as the base collector substrate material is its low thermal conductivity (K = 0.18 W/cm-K).

(4) Aluminum alloy type 3003-H14 with three surface preparations: (1) sand-blasted, (2) as-machined and (3) polished (Fig. 7b). The polished sample has the lowest emittance, followed by the as-machined and sandblasted samples, in that order. These samples were prepared for Alcoa (Aluminum Company of America) for treatment to produce their "low emissivity surface." Although this alloy will not withstand the 300°C temperature of the focused collector system, it may be useful in a flat plate collector system.

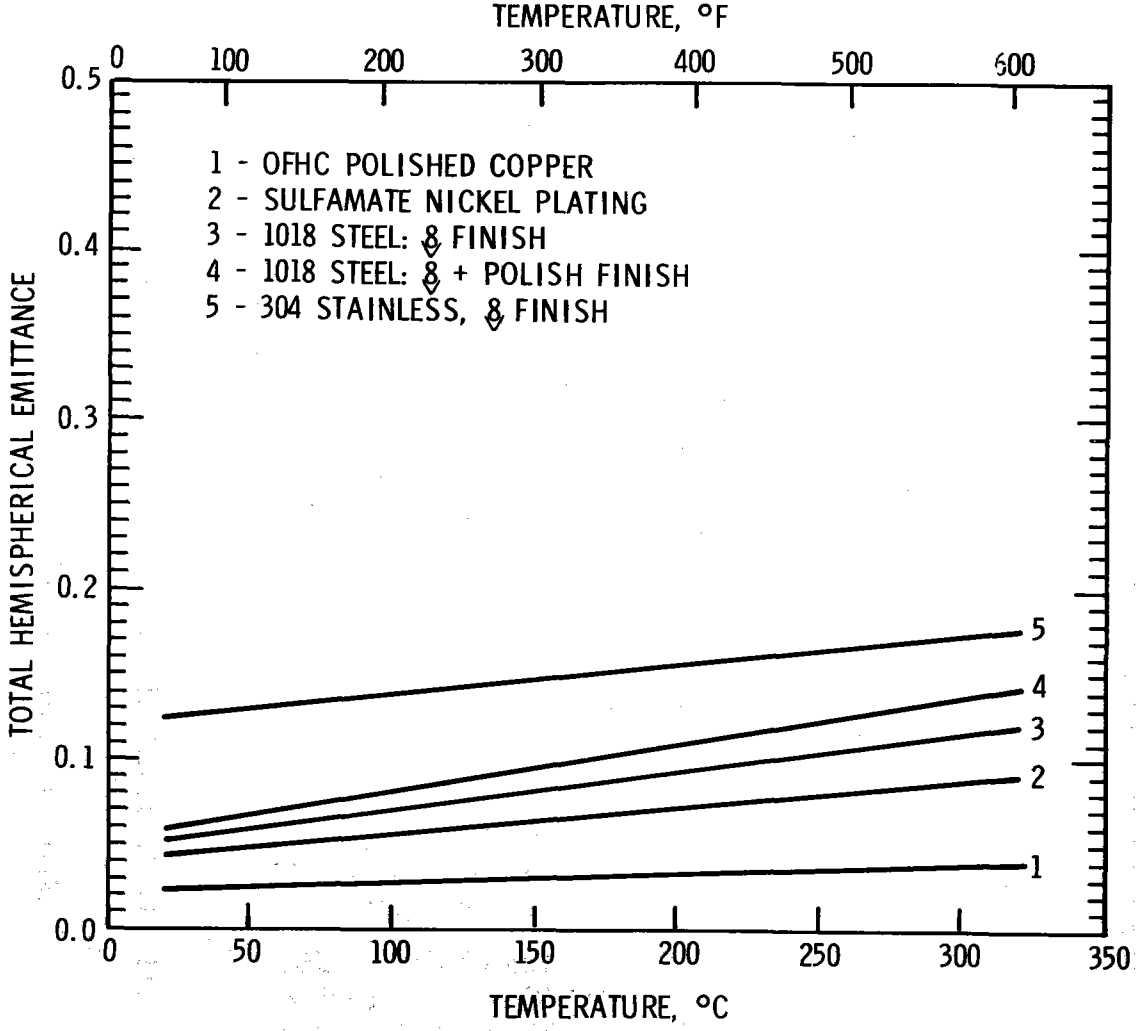

Figure 7a. Measured total hemispherical emittance values as a function of temperature for several metallic surfaces.

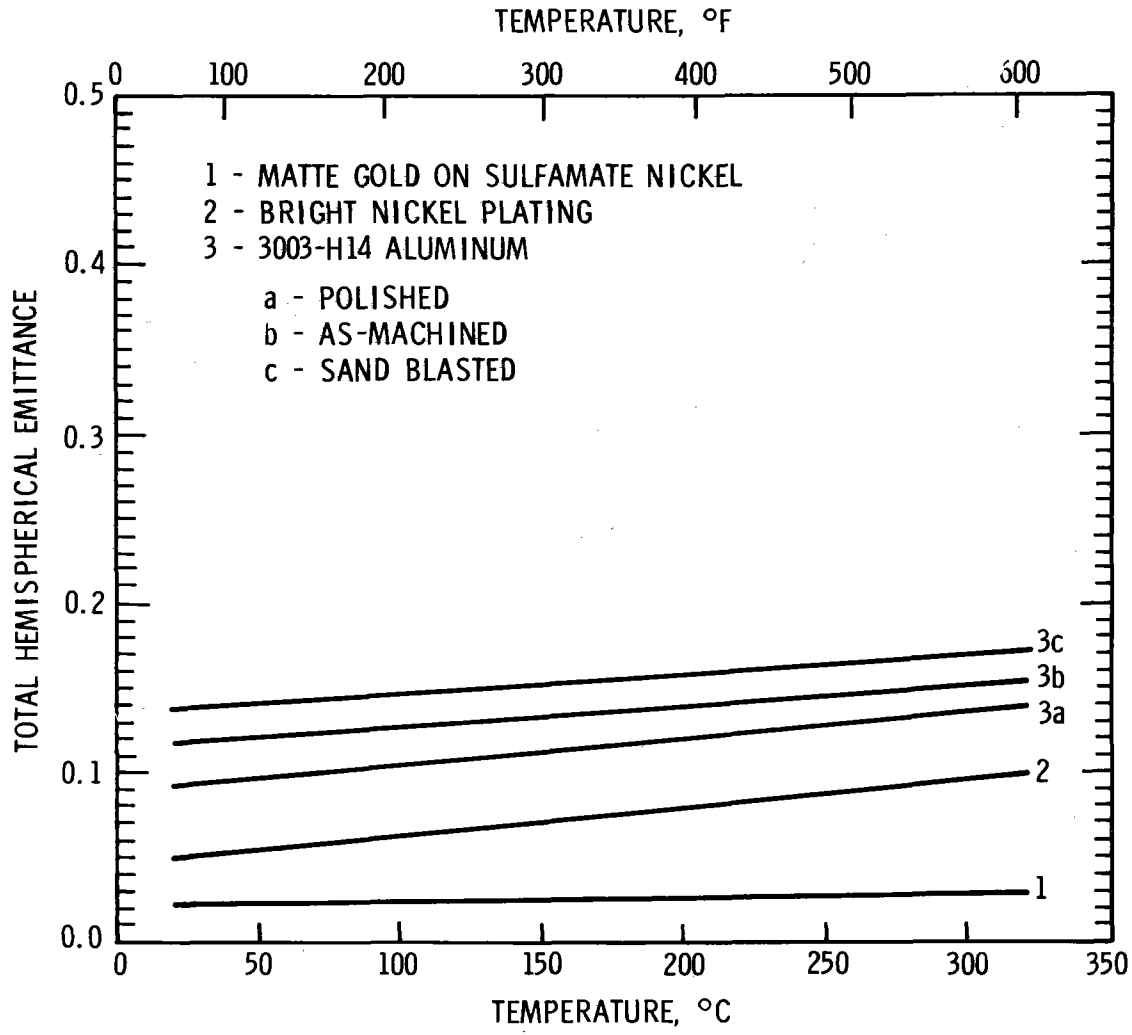

Figure 7b. Measured total hemispherical emittance values as a function of temperature for several metallic surfaces.

(5) A bright nickel plating, 0.1 to 0.2 mils thick, on a copper plating on 1018 steel (Fig. 1b). This metallic coating might be applied to the steel collector pipe both to protect the mild steel from oxidizing (rusting) and to provide a smoother surface. The emittance of this coating is less than 0.10 from 25°C to 300°C.

(6) A sulfamate nickel plating on 1018 steel substrates (Fig. 7a). Two coating thicknesses were studied: 0.0003" and 0.0030". The sulfamate nickel corresponds to a "dull" nickel plating. For both samples, the total emittance values as a function of temperature were identical, and, in fact, were the same as the total emittance of the bright nickel plating. There are two reasons for considering a sulfamate instead of a bright nickel plating on a collector pipe: (1) The solar absorptance of a thin coating (in particular, black nickel or chromonyx coatings) is increased while maintaining the same value for the total emittance; and (2) it is felt that the solar absorptance vs. incident angle profile will show less of a decrease with angle for the sulfamate nickel substrate than for the bright nickel substrate.

(7) A matte gold plating on a sulfamate nickel plated 1018 steel substrate (Fig. 7b). The gold plating has a total emittance of ~ 0.03 from 25°C to 300°C, which agrees with previously published data for gold,[16] and represents one of the lowest emittance samples measured. If this matte gold plating was used as the metallic substrate for an infrared transparent solar coating (i.e., black nickel, chromonyx, or PbS), the resulting sample would have a much lower emittance than the same solar coating on a sulfamate nickel substrate, for instance. However, because of the high solar reflectance of the gold substrate, the solar absorptance of such a sample may be less than the absorptance of the same coating on sulfamate nickel.

For the metallic substrates reported above, total hemispherical emittance values vary from 0.03 to 0.15 at 25°C and from 0.03 to 0.18 at 300°C. Therefore, on the basis of the emittance values, all these materials would be suitable as substrates for solar selective coatings.[17] The emittance values measured for polished copper, 304 stainless and electroplated gold agree with previous measurements within experimental uncertainties. In addition, the emittance of a rough surface is higher than the emittance of a polished surface for the same material, which is expected. However, the amount of increase is dependent upon the detailed character of the surface roughness, which is difficult to determine.[6]

Future Improvements

As indicated in the error analysis section, sample temperature measurement represented a substantial source of the overall emittance error. Therefore, a definite improvement would be obtained through the use of a more accurate thermometer. One candidate is a platinum resistance thermometer which can be used from -260 to 1000°C, is very accurate ($\pm$ 0.25°C), and is repeatable on temperature cycling to better than $\pm$ 0.1°C.[18] Such a thermometer would reduce the emittance error by more than a factor of 2.

In a focused collector, the solar selective coating will be deposited on a relatively small diameter (1" to 2") pipe.[17] It would be very desirable to be able to measure the emittance of coatings applied to actual collector pipe sections. The advantages of such a measurement would be to compare small laboratory samples to large production size samples, to check processing, electroplating or vacuum deposition techniques developed for tubular geometries as compared to flat plate geometries, as well as to provide emittance values for actual collector pipes. Such a measurement could be easily implemented with the present apparatus by using a circular heater that would fit inside the collector pipe section. The ends of the pipe could be closed off with a material of known total hemispherical emittance (plated bright nickel, for example). The measurement procedure used would be identical to the procedure developed for flat plate specimens.

Conclusions

With the present apparatus, the total hemispherical emittance of metallic samples can be measured from room temperature to over 300°C. The accuracy of the measurement varies from ± 0.01 to ± 0.045 emittance units depending upon the sample emittance and temperature. In particular, for emittance values below 0.30, the error is less than ± 0.02 emittance units. The modified steady-state calorimetric technique developed here (i.e., the delta-power method) allows for approximately six equilibrium temperatures to be obtained in two days for low emittance samples, and in one day for high emittance samples. In addition, the apparatus and experimental technique are easily adaptable to emittance measurements of collector pipe sections.

The total hemispherical emittance of several polished metallic substrates, suitable as base solar collector substrates, varied between 0.03 and 0.18 at 300°C. The emittance measured for a rough surface was generally higher than the emittance measured for a polished surface of the same material. However, for solar coating applications, the use of smooth surfaces to decrease emittance would have to be evaluated relative to the advantages of increased solar absorption by roughened surfaces.

References

1. R. M. Van Vliet, Coatings for the Aerospace Environment, ed. R. M. Van Vliet, USAF WADD-TR-60-773,(1961).

2. P. Moon, J. Franklin Inst. 230, 583 (1940).

3. M. M. Koltun, Geliotekhnika. 7, 70 (1971).

4. H. Tabor, Trans. of the Conf. on the Use of Solar Energy, Vol. II, Sec. A, (1955).

5. See J. P. Holman, Heat Transfer, Chapter 8, McGraw-Hill, New York (1963).

6. See Thermal Radiative Properties - Metallic Elements and Alloys, pp. 27a-29a, ed. Y. S. Touloukian and D. P. Dewitt, Plenum Press, N.Y. (1970).

7. J. P. Millard and E. R. Streed, Appl. Optics 8, 1485 (1969).

8. See Ref. 6 above, pp. 29a-42a.

9. W. B. Fussell, J. J. Trido and J. H. Henniger, Measurement of Thermal Radiation Properties of Solids, ed. J. C. Richmond, NASA-SP-31, p. 83 (1963).

10. For a complete discussion of Kirchhoff's Law, see Ref. 6, p. 7a.

11. See Thermal Radiative Properties (Coatings), pp. 533, ed. by Y. S. Touloukian, D. P. Dewitt, and R. S. Hernicz, Plenum Press, New York (1972), together with our own measurements to 300°C.

12. See Ref. 11, pp. 121, together with our own measurements to 300°C.

13. S. Dushman, Scientific Foundation of Vacuum Technique, J. Wiley and Sons, New York, (1949).

14. See Ref. 6, p. 138.

15. See Ref. 6, p. 1213.

16. See Ref. 6, p. 244.

17. W. H. McCulloch and G. W. Treadwell, Sandia Laboratories Energy Report, SAND-74 0124 (1974).

18. See for example, Bulletin 1011, Rosemount Engineering Co., (1973).

DISTRIBUTION:

Unlimited Release

A. Warren Adam
Sundstrand Electric Power
4747 Harrison Avenue
Rockford, Illinois 61101

J. D. Balcomb
Los Alamos Scientific Lab
Assistant Division Leader
for Analysis & Planning
Mail Stop 571
Los Alamos, New Mexico 87545

Richard Balzhizer
Office of Science & Technology
Executive Office of the President
Washington, D. C. 20506

Barber-Nichols Engineering
6325 West 55th Avenue
Arvada, Colorado 80002

Charles D. Beach
Westinghouse Georesearch Laboratory
8041 Baseline Road
Boulder, Colorado 80303

Jerry O. Bradley
Midwest Research Institute
425 Volker Blvd.
Kansas City, Missouri 64110

Floyd Blake
Martin Marietta Aerospace
Denver Division
P. O. Box 179
Denver, Colorado 80201

Karl W. Boer
Institute of Energy Conversion
University of Delaware
Newark, Delaware 19711

P. B. Bos
Manager, Solar Projects
Energy Projects Group
P. O. Box 92957
Aerospace Corp.
Los Angeles, California 90045

James C. Bresee
E463
Division of Applied Technology
USERDA
Germantown, Maryland 20767

Harold Bullis
Science Policy Division
Congressional Research Service
Library of Congress
Washington, D. C. 20540

J. O. Carnes
Southern Union Gas Company
Fidelity Union Tower Building
Room 1537
1507 Pacific Avenue
Dallas, Texas 75201

Ronal Larsen
Office of Technology Assessment
Old Immigration Building, Rm. 722
119 D St., NE
Washington, D. C. 20002

Commanding General
White Sands Missile Range
Attn: STEWS-TE-NT
Marvin Squires
White Sands Missile Range, NM 88002

John Martin
Argonne National Laboratory
9700 S. Cass Ave.
Argonne, Illinois 60439

J. R. Cotton, Chief
Reimbursable Activities Branch
US ERDA/ALO
Albuquerque, New Mexico 87115

Joe Guthrie
Enviro-Cynamics
3700 McKinney Ave
Dallas, Texas 75204

B. D. Daugherty
Southern Union Gas Company
8th and Silver SW
Albuquerque, New Mexico 87103

Jesse C. Denton
National Center for Energy
Management and Power
113 Towne Building
University of Pennsylvania
Philadelphia, Pennsylvania 19104

Gus Dorough
Deputy Director for Research &
Advanced Technology
Room 3E144/Pentagon Mail Stop 103
Washington, D. C. 20540

Solar Energy Application Lab
Colorado State University
Ft. Collins, Colorado 80521

H. Silha
University of Idaho
Moscoe, Idaho 83843

DISTRIBUTION (cont.)

Lou Werner
Divisiom of Applied Technology
Atomic Energy Commission, HQ
Germantown, Maryland 20767

Frank Zarb
Office of Management and Budget
Washington, D. C.

Sam Taylor
Federal Energy Administration
Washington, D. C.

Louis O. Elsaesser
Director of Research
Edison Electric Institute
90 Park Avenue
New York, New York 10016

Edward H. Fleming
Room E-479
Division of Applied Technology
Atomic Energy Commission
Germantown, Maryland 20767

Richard Hill
Federal Power Commission
441 G. Street, N.W. Room 4005
Washington, D. C. 20426

George Kaplan
National Science Foundation
1800 G. Street NW
Washington, D. C. 20550

Charles Kelber
Argonne National Laboratory
9700 South Cass Avenue
Argonne, Illinois 60439

D. K. Nowlin, Director
Special Programs Division
U.S. Atomic Energy Commission
Albuquerque, New Mexico 87115

Martin Prochnik
Deputy to the Science Advisor
U.S. Department of Interior
Room 5204
Washington, D. C. 20204

James E. Rannels
Division of Applied Technology
Atomic Energy Commission, HQ
Germantown, Maryland 20767

M. W. Rosenthal
Holifield National Laboratory
P. O. Box Y
Oak Ridge, Tennessee 37830

R. San Martin
New Mexico State University
Las Cruces, New Mexico 88001

R. Schmidt
Systems & Research Center
Honeywell Incorporated
2700 Ridgeway Road
Minneapolis, Minnesota 55413

G. Schreiber
Public Service Company
414 Silver Avenue, SW
Albuquerque, New Mexico 87103

J. W. Schroer, Chief
Special Projects Branch
USERDA/ALO
Albuquerque, New Mexico

Robert W. Scott
Manager, USERDA/SAO
Albuquerque, New Mexico 87115

Alan R. Siegel
Director, Environmental Factors & Public
Utilities Division
Department of Housing & Urban Development
Washington, D. C. 20410

F. M. Smits
Bell Laboratories
555 Union Boulevard
Allentown, Pennsylvania 18103

Dwain Spencer
Electric Power Research Institute
3412 Hillview Avenue
Palo Alto, California 94304

Ross Stickley
G. T. S. Sheldahl Co.
Northfield, Minnesota 55057

Pete Susey
American Gas Association
1515 Wilson Boulevard
Arlington, Virginia 22209

Ira Thierer
Southern California Edison
P. O. Box 800
2244 Walnut Grove Avenue
Rosemead, California 91770

U. S. Energy Research and Development
Administration
Division of Military Application
Attn: Major Gen. Frank A. Camm
Asst. Gen. Manager for Military Appl.
Washington, D. C. 20545

DISTRIBUTION (cont'd)

Lorin L. Vant-Hull
Dept. of Physics
University of Houston
3801 Cullen Boulevard
Houston, Texas 77004

Michael Wahlig
Lawrence Berkeley Laboratory
Bldg. 50A, Room 6121
University of California
Berkeley, California 94720

W. A. Cross
Attn: M. Wilden
Dept. of Mechanical Engineering
University of New Mexico
Albuquerque, New Mexico 87106

Karl Willenbrock
Director, Institute for Appl. Tech.
National Bureau of Standards
Room B-112, Tech (400.00)
Washington, D. C. 20234

Leanard S. Raymond
Optical Sciences Center
Tucson, Arizona 85721

S. Moore
Q-DOT
Los Alamos Scientific Laboratory
Los Alamos, New Mexico 87545

1543 W. H. McCulloch
5000 A. Narath

Attn: J. K. Galt - 5100
E. H. Beckner - 5200
A. Y. Pope - 5600
J. H. Scott - 5700

5710 G. E. Brandvold
5712 R. H. Braasch (25)
5712 B. J. Petterson
5712 J. A. Leonard
5712 G. W. Treadwell
5717 R. P. Stromberg
5800 L. M. Berry

Attn: R. G. Kepler - 5810
R. L. Schwoebel - 5820
M. J. Davis - 5830

5834 D. M. Mattox
5834 R. R. Sowell
5840 D. M. Schuster
5842 R. C. Heckman
5842 R. P. Pettit (15)
5844 B. L. Butler
5844 F. P. Gerstle
5846 E. K. Beauchamp
5847 C. H. Karnes
8184 A. C. Skinrood
8424 H. R. Sheppard
9412 R. K. Peterson

3141 Library (5)
3151 Tech. Publications (3)
3171-1 R. P. Campbell (25)
(For ERDA-TIC)
8266 Library (2)

Org.	Bldg.	Name	Rec'd by*	Org.	Bldg.	Name	Rec'd by*
8184		AC Skinrood					

*Recipient must initial on classified documents.